Electronic structure and magnetism in doped semiconducting half-Heusler compounds

2005 J. Phys.: Condens. Matter 17 5037

(http://iopscience.iop.org/0953-8984/17/33/008)

INSTITUTE OF PHYSICS PUBLISHING JOURNAL OF PHYSICS: CONDENSED MATTER

J. Phys.: Condens. Matter **17** (2005) 5037–5048 doi:10.1088/0953-8984/17/33/008

Electronic structure and magnetism in doped semiconducting half-Heusler compounds

B R K Nanda and I Dasgupta[1]

Department of Physics, Indian Institute of Technology Bombay, Powai, Mumbai 400076, India

E-mail: dasgupta@phy.iitb.ac.in

Received 24 March 2005, in final form 23 June 2005
Published 5 August 2005
Online at stacks.iop.org/JPhysCM/17/5037

Abstract

We have studied in detail the electronic structure and magnetism in M (Mn and Cr)-doped semiconducting half-Heusler compounds FeVSb, CoTiSb and NiTiSn ($XY_xM_{1-x}Z$) in a wide concentration range using the local-spin density functional method in the framework of the tight-binding linearized muffin tin orbital method (TB-LMTO) and supercell approach. Our calculations indicate that some of these compounds are not only ferromagnetic but also half-metallic and may be useful for spintronics applications. The electronic structure of the doped systems is analysed with the aid of a simple model where we have considered the interaction between the dopant transition metal (M) and the valence band X–Z hybrid. We have shown that the strong X-d–M-d interaction places the M-d states close to the Fermi level with the M-t_{2g} states lying higher in energy in comparison to the M-e_g states. Depending on the number of available d electrons, ferromagnetism is realized provided that the d manifold is partially occupied. The tendencies toward ferromagnetic (FM) or antiferromagnetic (AFM) behaviour are discussed within Anderson–Hasegawa models of super-exchange and double-exchange. In our calculations for Mn-doped NiTiSn, the strong preference for FM over AFM ordering suggests a possible high Curie temperature for these systems.

1. Introduction

Spin-based electronics or spintronics is currently an active area of research because it provides a possibility to integrate electronic, opto-electronic and magneto-electronic multifunctionality on a single device exploiting both the spin as well as the charge degree of freedom of an electron. The half-metallic ferromagnets having only one electronic spin direction at the Fermi energy resulting in 100% spin-polarization and ferromagnetic semiconductors where magnetic and semiconducting properties can be controlled and tuned are suggested to be suitable candidates for spintronic applications. The recent interest in ferromagnetic semiconductors

[1] Author to whom any correspondence should be addressed.

0953-8984/05/335037+12$30.00

for spintronic applications is spurred by the pioneering work by Ohno and co-workers [1], in the late 1990s, showing that a ferromagnetic Curie temperature as high as 110 K can be achieved in Mn-doped GaAs, demonstrating the feasibility that ferromagnetic property can be incorporated in traditional semiconductors. This work has stimulated vigorous experimental as well as theoretical activity in diluted magnetic semiconductors (DMSs). As a result, on the experimental front, ferromagnetism in diluted magnetic semiconductors, in some cases with T_c close to room temperature, have been reported for Mn-doped GaP [2], Mn-doped chalcopyrite $CdGeP_2$ [3] and Mn-doped GaN [4, 5]. Ferromagnetism has also been reported for oxide-based diluted magnetic semiconductors such as Co-doped TiO_2 [6], SnO_2 [7] and $La_{1-x}Sr_xTiO_{3-\delta}$ [8].

The present theoretical understanding of ferromagnetism in DMSs is very limited. The widely accepted model Hamiltonian [9] for an Mn-doped DMS, e.g. $Ga_{1-x}Mn_xSb$, considers the impurity state bound to Mn ion to be shallow acceptors formed from the host material and the interaction between the Mn impurity spin orientations to be mediated by valence band holes. The exchange interaction between the localized transition metal impurities is suggested to be RKKY like, and it has been argued that such a model can capture salient features of the diluted magnetic semiconductors. The other possible mechanism that can stabilize ferromagnetism in DMSs is suggested to be Zener's p–d exchange [10]. On the other hand, the first principles calculations suggest that the Mn-induced hole can have significant 3d character. In the series [11] Mn-doped GaN $\rightarrow$ GaP $\rightarrow$ GaAs $\rightarrow$ GaSb the hole generated by introducing Mn in GaN is found to have significant 3d character, while in GaSb the hole is found to have primarily host character. Further, the first principles calculations suggest that ferromagnetism is stabilized by a kinetic energy driven mechanism either by hybridization-induced negative exchange splitting [12] or double exchange [13], depending on the nature and the location of the holes.

The discussion in the preceding paragraph suggests that the mechanism behind ferromagnetism in DMSs is still far from complete. It also raises the important questions whether any transition metal (TM)–semiconductor combination will result in ferromagnetism and what are the relevant energetics that govern the interaction of the transition metal with the host resulting in ferromagnetism. To understand some of these issues the current research effort in spintronics materials is also directed toward the search for potential DMS hosts. Recently it was found experimentally [14] that the semiconducting tetradymite structure material Sb_2Te_3 acts as a DMS with $T_c \simeq 20$ K when doped with a few per cent of V atoms. Similarly, a recent, first principles calculation, [15] indicated that transition-metal-doped SiC may be ferromagnetic with T_c very close to room temperature. In the present work we have considered semiconducting half-Heusler systems as a potential DMS host.

The half-Heusler compounds, with the general formula XYZ, where X and Y are transition metals and Z is a sp-valent element, have been a subject of continuous attention because of their variety of novel magnetic properties ranging from antiferromagnets [16], half-metallic ferromagnets [17], weak ferromagnets, Pauli metals, semimetals [18] to semiconductors [19]. In particular, the half-metallic semi-Heusler alloys can be attractive for spintronics applications due to their relatively high Curie temperature and similarity of the crystal structure to the zinc-blende structure which is adopted by a large number of semiconductors like GaAs, ZnSe, and InAs. In the present work, inspired by DMSs, we have examined in detail the electronic structure of 18 valence electron semiconducting half-Heusler alloys FeVSb, CoTiSb and NiTiSn when doped with transition-metal impurities Mn and Cr. The electronic structure of Mn-doped semiconducting half-Heusler alloys have also been investigated in the framework of KKR-CPA calculations [21]. The doped Heusler systems has also been a subject of interest due to the possibility of realizing half-metallic antiferromagnetism [20].

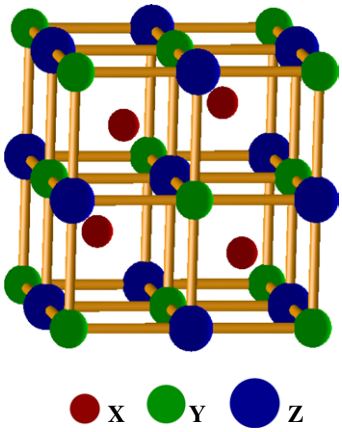

Figure 1. The cubic half-Heusler structure.
(This figure is in colour only in the electronic version)

Half-metallic antiferromagnets are half-metallic systems with vanishing macroscopic moment. Our calculations for the doped semiconducting half-Heusler systems suggest that for impurity concentrations as low as 3% some semiconducting half-Heusler systems are transformed to half-metallic ferromagnets, possibly with high Curie temperature.

The rest of the paper is organized as follows. In section 2 we describe the crystal structure and the computational details. A detailed analysis of the electronic structure and magnetism of doped Heusler systems is carried out in section 3. Finally, in section 4 we present our conclusions.

2. Structure and computational details

The half-Heusler compounds XYZ crystallize in the face centred cubic structure with one formula unit per unit cell, as shown in figure 1. The space group is $F4/3m$ (No 216). For the semiconducting half-Heusler systems considered here the higher-valent transition elements Fe, Co and Ni represent X while the lower-valent transition element V, Ti represent Y, and Sb/Sn represent Z. In the conventional stable structure Y and Z atoms are located at 4a (0, 0, 0) and 4b $(\frac{1}{2}, \frac{1}{2}, \frac{1}{2})$ positions, forming the rock-salt structure arrangement. The X atom is located in the octahedral coordinated pocket, at one of the cube centre positions 4c $(\frac{1}{4}, \frac{1}{4}, \frac{1}{4})$, leaving the other position 4d $(\frac{3}{4}, \frac{3}{4}, \frac{3}{4})$ empty. When the Z atomic positions are empty the structure is analogous to the zinc-blende structure, which is common for a large number of semiconductors.

In order to study the effect of Mn and Cr impurities (M) in semiconducting half-Heusler systems (i.e. to simulate the effect of doping) we have constructed supercells with size dependent on the percentage of M doping. In each supercell we have replaced either one or two Y atoms by M atoms. For the two impurities embedded in the supercell we have studied the electronic structure of these doped systems both as a function of orientation of one M atom with respect to the other as well as of distance between the two M atoms. Further embedding a pair of impurity atoms also allowed us to study the interaction between a pair of M moments. The largest supercell chosen was 64 times the original unit cell and consisted of 192 (256) atoms (including the empty spheres) to simulate 3.125% concentration for a pair of M atoms. The size of the supercell was chosen to ensure that the separation between the impurities is much smaller in comparison to the dimension of the supercell.

All the electronic structure calculations reported in this work have been performed using the self-consistent tight-binding linear muffin-tin orbital (TB-LMTO) method with the atomic

sphere approximation (ASA) and the combined correction [22]. TB-LMTO-ASA has been established as an intelligible, fast and accurate method to understand electronic structure and chemical bonding for a large class of solids, including systems with pronounced directional bonding [23, 24]. Recently we have employed [25] the TB-LMTO-ASA method coupled with the crystal orbital Hamiltonian population (COHP) [26] for an energy-resolved visualization of chemical bonding in half-Heusler systems. Self-consistent TB-LMTO-ASA calculations are done in the framework of the LDA [27]. We have also checked our calculations within the generalized gradient approximation (GGA) [28] and the results are found to be very similar to the LDA results. The space filling in the ASA is achieved by inserting empty spheres in the cube centre positions ($\frac{3}{4}$, $\frac{3}{4}$, $\frac{3}{4}$) and by inflating the atom-centred non-overlapping spheres. The atomic radii are chosen in such a way that there is negligible charge on the empty spheres and the overlap of the interstitial with the interstitial, atomic with atomic, and interstitial with the atomic spheres remains within the permissible limit of the ASA. The basis set of the self-consistent electronic structure calculation includes X, Y, M (s, p, d) and Z (s, p) and the rest are downfolded. A [16, 16, 16] k-mesh has been used for self-consistency for all the calculations except for largest supercell where we have used an [8, 8, 8] k-mesh. All the k-space integration was performed using the tetrahedron method [29]. Experimental lattice parameters 5.82 Å, 5.88 Å [19], 5.924 Å [30] for FeVSb, CoTiSb and NiTiSn respectively were used for the doped structure and structural relaxations around the impurities were not included in the present calculations.

3. Results and discussions

3.1. Paramagnetic electronic structure of $XY_xM_{1-x}Z$

In this section, we shall present the results of the TB-LMTO-ASA electronic structure calculations for the Mn-doped semiconducting half-Heusler systems in the unstable paramagnetic phase. We have considered three narrow gap semiconducting half-Heusler systems, FeVSb, CoTiSb and NiTiSn, as the host material. In each system the lower-valent transition element (V and Ti) is substituted with M (Mn, Cr) with concentration ranging from 25% to 3.125%. Our calculations [31] suggest that M substitution at other sites, namely X (Fe, Co, Ni), Z (Sn, Sb) and the voids, is energetically unfavourable. This result is consistent with recent KKR-CPA calculations on some of these systems [21]. In the first and second rows of figure 2 we have displayed the total density of states (DOS) for the semiconducting half-Heusler hosts and the doped systems $XMn_{0.25}Y_{0.75}Z$ in the paramagnetic phase, respectively. Before we discuss the electronic structure of the doped systems we shall briefly discuss the electronic structure of the host materials.

The characteristic feature of the electronic structure of the undoped compounds (XYZ, valence electron count (VEC) $=$ 18, semiconducting) shown in the first row of figure 2 is a pair of bonding and antibonding states separated by a gap. The bonding states below the gap are predominantly of X character while the antibonding states are of Y character. The semiconducting gap is a consequence of the covalent hybridization of the higher-valent transition element X with the lower-valent transition element Y. Further, the bonding states are well separated from the Sb-p states in FeVSb and CoTiSb by a small p–d gap, while the Sb-s states are lying far below the chosen scale of the figure. In NiTiSn, the Sn-p states lie higher in energy compared to Sb, overlapping with the bonding complex, and therefore the p–d gap does not exist. Again the Sn-s states are far below the chosen scale of the figure. So below the d–d gap there are 9 bands (4 Z s + p, and 5 predominantly X-d) which in the paramagnetic phase can accommodate 18 electrons of both spins. Hence with 18 valence electrons all

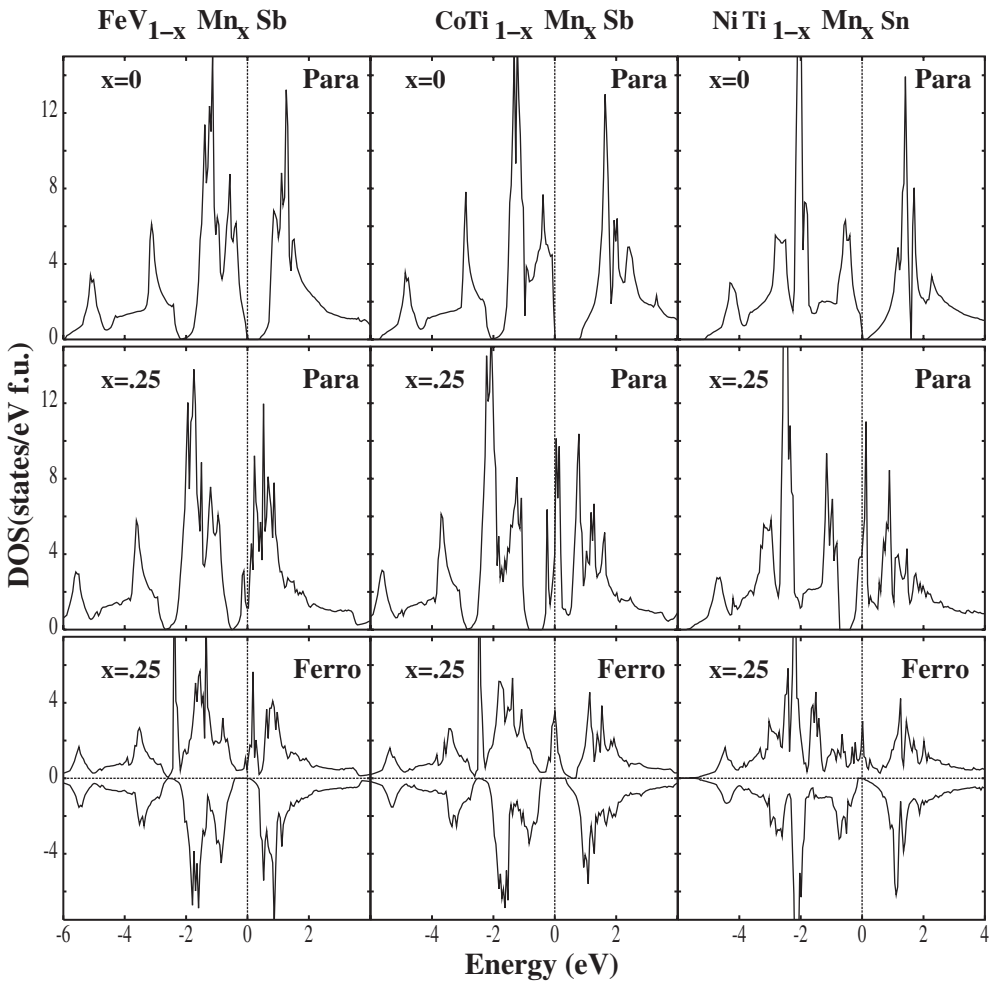

Figure 2. Density of states for formula unit for $FeV_{1-x}Mn_xSb$ (first panel), $CoTi_{1-x}Mn_xSb$ (second column) and $NiTi_{1-x}Mn_xSn$ (third column). The first row shows the paramagnetic density of states of the semiconducting compound ($x = 0.0$). The second and third rows respectively show the paramagnetic and ferromagnetic density of states of the Mn-doped compound ($x = 0.25$). All energies are w.r.t. the Fermi energy.

the s–p and d states below the d–d gap are saturated, resulting in bond orbitals with strong directionality and bonding. This explains why half-Heusler systems with 18 valence electrons are semiconductors [25, 32]. We note that the presence of the Z (Sb/Sn) atom which provides a channel to accommodate some transition-metal d electrons in addition to its s–p electron is therefore crucial for the stability of these systems. For the half-Heusler systems with more than 18 valence electrons the antibonding states are occupied, and if the DOS at the Fermi level is high then the paramagnetic state is no longer stable and the stability can be achieved by developing a magnetic order. We have recently shown [25] that the presence of a gap in the paramagnetic phase promotes half-metallic ferromagnetism for systems with VEC > 18 as has been realized for example in NiMnSb.

We shall now consider the doped systems in the paramagnetic phase shown in the second row of figure 2. In the doped systems, replacing Ti/V with Mn puts an additional three/two

Table 1. Magnetic moments (in μ_B) of doped half-Heusler compounds.

Host compound	Impurity M	Impurity Conc. (%)	Total mag. mom.	M mag. mom.	p–d hybrid (X + Z) mag. mom.	Y + E mag. mom.
FeVSb	Mn	25.00	2.00	2.67	−0.98	0.31
		12.50	2.00	2.64	−1.15	0.51
		6.250	2.00	2.61	−1.34	0.73
		3.125	2.00	2.58	−1.45	0.87
CoTiSb		25.00	3.00	3.25	0.05	−0.30
		12.50	3.00	3.24	−0.05	−0.19
		6.250	3.00	3.24	−0.16	−0.08
		3.125	3.00	3.22	−0.27	0.05
NiTiSn		25.00	3.00	3.44	0.04	−0.48
		12.50	3.00	3.41	0.07	−0.48
		6.250	3.00	3.43	0.06	−0.49
		3.125	3.00	3.40	0.01	−0.41
FeVSb	Cr	25.00	1.00	1.68	−0.95	0.27
		12.50	1.00	1.54	−1.02	0.48
		6.250	1.00	1.37	−1.12	0.75
CoTiSb		25.00	2.00	2.58	−0.49	−0.09
		12.50	2.00	2.53	−0.50	−0.03
		6.250	2.00	2.56	−0.69	0.13
NiTiSn		25.00	1.97	2.77	−0.25	−0.55
		12.50	1.85	2.64	−0.23	−0.56
		6.250	1.51	2.40	−0.25	−0.64

electrons in the system per Mn (VEC $>$ 18); as a consequence the systems are no longer semiconducting. This is reflected in the DOS for 25% Mn-doped compound as a deep donor level produced by the addition of Mn impurities and the Fermi level lies on this predominantly Mn-driven state. It is clear from the DOS peaks that the paramagnetic phase has a Stoner instability and a ferromagnetic state with finite moment is likely to be energetically favourable to the paramagnetic state. The calculated DOS at the Fermi level $D(E_F)$ is 2.21, 6.2 and 7.5 states/eV/Mn for 25% Mn-doped FeVSb, CoTiSb and NiTiSn, respectively. Assuming the usual value of the Stoner interaction parameter $I_{Mn} = 0.75$ eV leads to $D(E_f)I \simeq 1.7, 4.6,$ 5.6, suggesting Stoner instability, particularly strong for Mn-doped NiTiSn, and considerable energy gain via spin polarization.

3.2. Spin-polarized calculations

Figure 2 (third row) displays the spin-polarized DOS for the 25% Mn-doped compound in the semiconducting host. From the figure we gather that the doped systems are not only ferromagnetic but also half-metallic, sustaining an integral moment of 3 μ_B for Mn in NiTiSn, CoTiSb and 2 μ_B in FeVSb (see table 1). Interestingly the defect states are screened metallically by the majority states, so the number of minority states does not change. The excess charges $\Delta z = 3, 3, 2$ per Mn in NiTiSn, CoTiSb and FeVSb respectively are accommodated in the majority spin channel, resulting in electronic states appearing as a new peak in the gap, which are primarily of Mn character. Hence the charge which is in excess of $n \times 18$ (n = size of the supercell) appears as a magnetic moment satisfying the 18-electron rule suggested for half-Heusler systems with VEC $>$ 18 [32].

We shall now discuss in detail the role of diluted magnetic impurities (Mn and Cr) in the three semiconducting hosts. In each case the lower-valent transition element Y has been

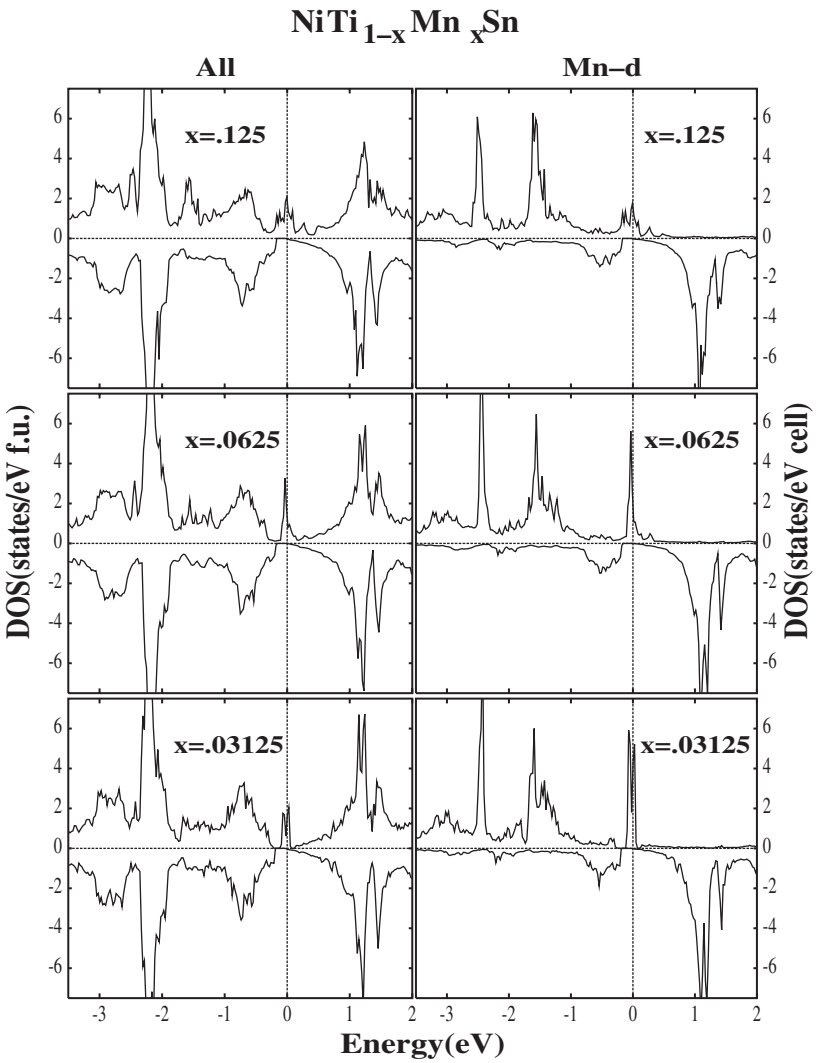

Figure 3. Spin-polarized density of states for $NiTi_{1-x}Mn_xSn$ ($x = 12.5\%$, 6.25%, 3.125%). In the left column the total density of states per formula unit is plotted while in the right column the Mn-d states per cell are plotted. All energies are w.r.t. the Fermi energy.

replaced with M(Mn/Cr) $XY_xM_{1-x}Z$ with $x = 12.5\%$, 6.25%, and 3.125%. For the purpose of discussion we have chosen a representative compound ($NiTi_{1-x}Mn_xSn$); however, our discussions holds for the other compounds as well. In figure 3 we have displayed the total DOS for one formula unit and the site projected Mn DOS for concentration $x = 12.5\%, 6.25\%$, and 3.125%. We gather from the total DOS that all the systems are half-metallic ferromagnets. When Mn is substituted for Ti, the additional three electrons per Mn are accommodated in the majority spin channel, producing Mn-derived states in the gap while the minority states remain nearly unchanged. The width of the impurity states, which is a consequence of the hybridization with the transition elements (Ni, Ti) and Sn, decreases when the concentration of the impurity M is low. We also note that the Mn-derived states are partially filled. Further,

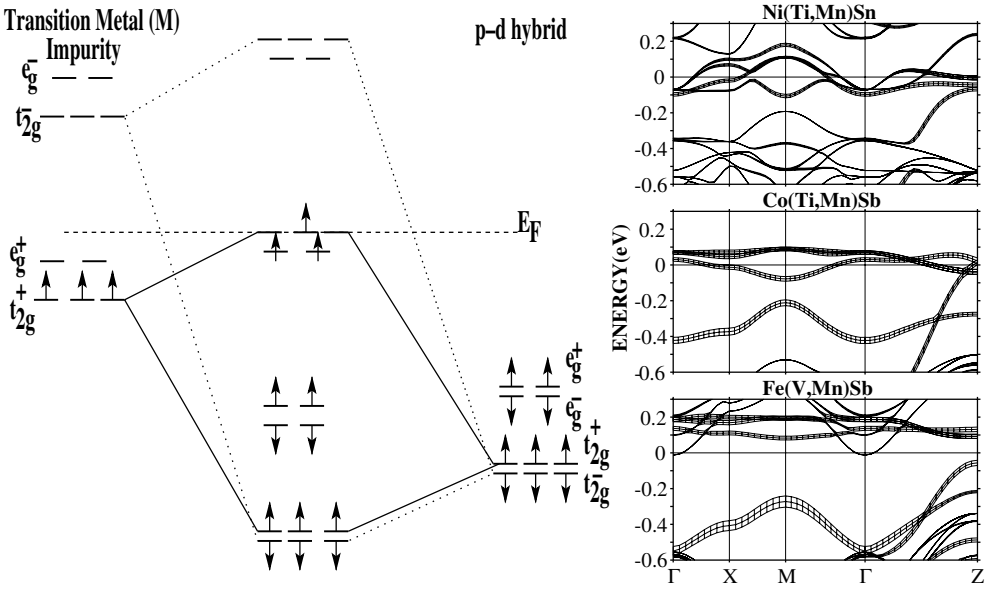

Figure 4. The gross features of the electronic structure and genesis of magnetism are shown through an energy level diagram in the left, and in the right the Mn-d characters (fat bands) are plotted for Ni(Ti, Mn)Sn, Co(Ti, Mn)Sb and Fe(V, Mn)Sb with 6.25% impurity concentrations. All energies are w.r.t. the Fermi energy.

we gather from the Mn partial DOS that there are sharp Mn-derived crystal field resonances deep in the valence band.

A Ti vacancy in NiTiSn creates holes in the Ni-d–Sn-p valence band hybrid due to depletion of four electrons per Ti, leaving the Ni-d–Sn-p dangling bonds unsaturated. When Mn, having seven valence electrons, is substituted, four electrons are utilized to saturate the dangling bonds and the additional three electrons, responsible for the magnetic properties, are accommodated in the high-spin state in the majority spin channel. This distribution of the Mn electrons results in crystal field resonances deep in the valence band, in addition to the partially filled impurity-derived states in the gap in the majority spin channel.

The gross feature of the electronic structure and magnetism in transition-metal-doped semiconducting half-Heusler compounds can be understood by invoking a simple model, where we consider the interaction between the dopant transition metal M and the valence band X–Z hybrid. Our simple model is schematically presented in figure 4. In view of the strong d–d interaction, the valence band hybrid to a first approximation is primarily of X-d character, which is split into t_{2g} and e_g levels by the crystal field. After acquiring transition-metal M electrons it is full and weakly spin split, as illustrated in figure 4 (right panel). On the other hand the transition-metal M-d levels are energetically shallower compared to the valence band hybrid. These levels are crystal field split as well as appreciably exchange split, as shown in figure 4 (left panel). The result in the presence of hybridization is shown in the central panel of the figure. Since the X atoms are arranged tetrahedrally to the M atoms strong X-t_{2g}–M-t_{2g} interaction is favoured with relatively weaker e_g–e_g interaction. The up (+) and down (−) spin states on the transition-metal atoms therefore interact via spin-conserving hopping interactions and form a set of bonding–antibonding states for each spin channel, as shown in the central panel of figure 4. We note from the central panel strong X-t_{2g}–M-t_{2g} hybridization places the transition-metal M-t_{2g} levels above the e_g levels, and the relative positions of these levels is

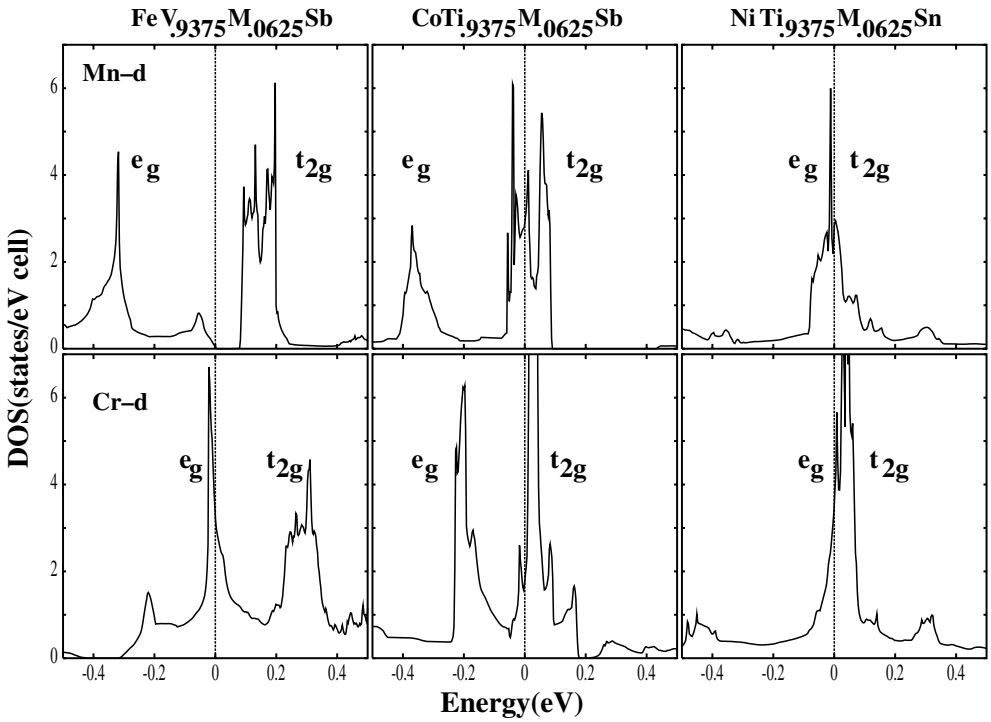

Figure 5. Spin-up Mn-d (top) and Cr-d (bottom) density of states for the doped compounds with 6.25% concentration. All energies are w.r.t. the Fermi energy.

governed by the strength of the X-t_{2g}–M-t_{2g} hybridization. We note from the M projected band structure (fat bands) shown in figure 4 (right) that the bands close to the Fermi level are partially filled Mn-d bands, as expected. We have recently shown [25] with the aid of a tight-binding analysis that this hybridization depends on the relative position of the transition elements X and M in the periodic table. As a consequence Fe–M hybridization > Co–M hybridization > Ni–M hybridization. This is further illustrated in figure 5, where we have displayed the M (Mn/Cr) projected partial DOS in a narrow energy range about the Fermi level for $XY_xM_{1-x}Z$, with $x = 6.25\%$ (only the spin-up channel is shown as the spin-down channel is empty in this energy range). We note from the figure that although the e_g and t_{2g} states are well split in Mn-doped FeVSb, the splitting decreases for CoTiSb, and is very small for Mn-doped NiTiSn, where the states are overlapping. So for Mn-doped NiTiSn the additional three electrons progressively fill up the overlapping e_g and t_{2g} levels, with the t_{2g} partially empty. The same is true for Mn-doped CoTiSb, while the e_g states are completely full for Mn-doped FeVSb (see figure 5). For the Cr-doped systems the splitting is very small for all semiconducting hosts, leaving the Cr-d states partially empty. The results of our calculations for the different hosts are summarized in table 1. We find from table 1 that the magnetic moment of M (Mn and Cr) remains almost the same with the concentration variation of M, with the only exception being Cr-doped FeVSb. This insensitivity of magnetic moment with concentration is a signature of localized d states of Mn and Cr. The localization comes from the fact that although the d electrons of M are itinerant, the spin-down electrons are almost excluded from the M site. Further, in all cases (except Cr-doped NiTiSn) the total moment is always integer, indicating a half-metallic solution.

Table 2. Magnetic moments in μ_B and ΔE (E_{FM}–E_AFM) for double impurity.

Host compound	Impurity Mn conc. (%)	FM total per Mn	Mn	AFM total	Mn	ΔE per Mn (meV)
FeVSb	25	2.00	2.64	0.00	2.65	−71.4
	12.5	2.00	2.60	0.00	2.57	−39.2
	6.25	2.00	2.56	0.00	2.56	−12.8
CoTiSb	25	3.00	3.22	0.00	3.28	−283.1
	12.5	3.00	3.21	0.00	3.22	−140.9
	6.25	3.00	3.21	0.00	3.16	−152.5
NiTiSn	25	3.00	3.36	0.00	3.48	−282.9
	12.5	3.00	3.36	0.00	3.43	−179.3
	6.25	3.00	3.32	0.00	3.38	−243.0

Finally, we have addressed the issue of the tendencies towards ferromagnetic or antiferromagnetic ordering in these systems. For this purpose we have performed spin-polarized density functional calculations with (i) two M spins parallel to each other, the ferromagnetic configuration, (ii) two M spins antiparallel to each other, the antiferromagnetic configuration. In order to understand the trends we have considered the hosts NiTiSn, CoTiSb and FeVSb doped with Mn; our results are summarized in table 2.

The stability of such a configuration in the context of diluted magnetic semiconductors is usually discussed in the framework of the Anderson–Hasegawa model [33]. If the M 3d orbital is partially occupied, in that case the 3d electrons in the partially occupied M orbitals are allowed to hop to the neighbouring M 3d orbitals, provided that the neighbouring M ions have parallel magnetic moments. As a result, the d electrons lower their kinetic energy by hopping in the ferromagnetic state. This is the so-called double exchange mechanism. However, if the transition metal M d orbitals are full then this reduction via hopping is not possible, and the energy is lowered by super-exchange, which requires the neighbouring spins to be antiparallel. In view of this it is expected that Mn-doped NiTiSn with partially occupied d levels should be ferromagnetic while Mn-doped FeVSb with empty t_{2g} orbitals should favour antiferromagnetic arrangement of spins. The total energy difference between FM and AFM configuration displayed in the last column of table 2 favours strong ferromagnetism for Mn-doped NiTiSn and CoTiSb and is consistent with the Anderson–Hasegawa model, while for Mn-doped FeVSb instead of expected AFM, the ferromagnetic state is found to be stable, although the energy difference ΔE is very small. For the cases where the e_g and t_{2g} states are nearly overlapping and the number of d electrons is less than five, so that the d manifold is only partially occupied, ferromagnetism is always stabilized. Finally, in figure 6 we have plotted ΔE as a function of Mn–Mn separation in the unit cell for Mn-doped FeVSb and NiTiSn. This difference in energy ΔE is also a measure of interatomic exchange interaction, and in the framework of mean-field theory is also proportional to T_c. Although ΔE is positive for both cases, it is very small for Mn-doped FeVSb, suggestive of the fact that ferromagnetism may not be sustained in this compound. This is consistent with the Anderson–Hasegawa model. Appreciable ΔE for Mn-doped NiTiSn suggests not only ferromagnetism for this compound but also appreciable T_c. Further, ΔE decreases sharply with distance, suggesting that the double exchange mediated ferromagnetic interaction in these systems is short ranged. A similar finding has been reported for Mn-doped GaN [34], where it has been suggested that short range interactions indicate the formation of Mn clusters within a short radial distance and might lead to a high value of T_c in these systems.

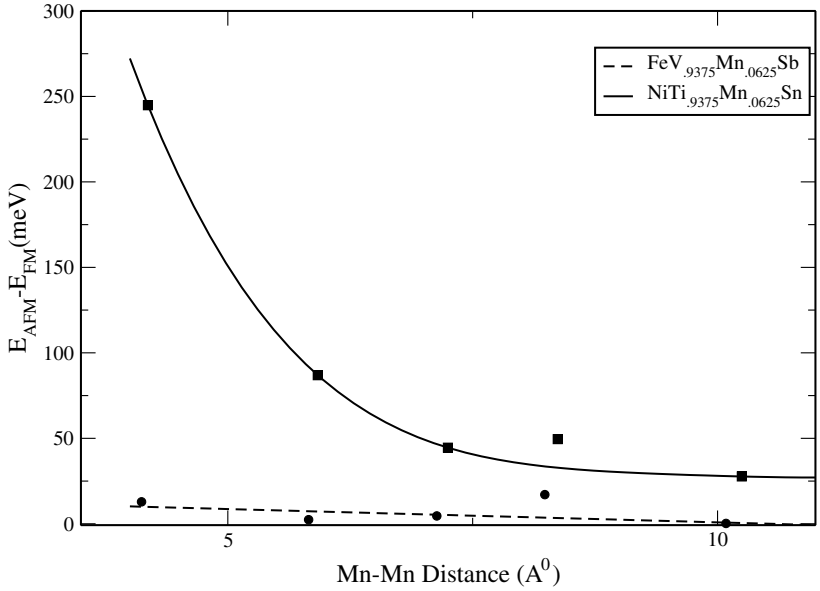

Figure 6. Energy difference between the AFM and FM phase ΔE $(=E_{\mathrm{AFM}} - E_{\mathrm{FM}})$ w.r.t. the Mn–Mn distance for $FeV_{0.9375}Mn_{0.0625}Sb$ and $NiTi_{0.9375}Mn_{0.0625}Sn$.

4. Summary and conclusions

We have studied in detail the electronic structure and magnetism in Mn- and Cr-doped semiconducting half-Heusler systems, namely FeVSb, CoTiSb and NiTiSn, for a wide concentration range. The characteristic feature of the electronic structure is a deep defect state of predominantly Mn/Cr character, in the majority spin channel. The ferromagnetism in this systems can be understood within the Anderson–Hasegawa model, which promotes ferromagnetism for partially filled d states. The electronic structure of the doped systems is analysed in the framework of a simple model where we have considered the interaction between the dopant transition metal M and the valence band X–Z hybrid. We have shown that strong X-t_{2g} and M-t_{2g} interactions place the M-d sates close to the Fermi level, with the t_{2g} states lying higher in energy in comparison to the e_g states. Further, the splitting of the d levels is not only governed by the local crystal field but also by the strength of hybridization between X-t_{2g} and M-t_{2g} sates. Depending on the number of available d electrons, ferromagnetism is realized, provided that the d manifold is partially empty, as suggested by the Anderson–Hasegawa model. We have also addressed the issue of the tendencies toward ferromagnetic or antiferromagnetic ordering in these systems. Our calculations suggest that the double exchange mediated ferromagnetism in these systems is short ranged. Further, the strong preference for ferromagnetic ordering over antiferromagnetic ordering in Mn-doped NiTiSn indicates it to be a half-metallic ferromagnet, possibly with a high Curie temperature. Based on these theoretical predictions it will be interesting to investigate these systems experimentally.

Acknowledgments

We thank S D Mahanti for useful discussions. BRKN thanks CSIR, India, for a research fellowship (SRF). The research is funded by CSIR (No 03(0931)/01/EMR-II)

References

[1] Ohno H 1998 *Science* **281** 951
[2] Theodoropoulou N and Hebard A F 2002 *Phys. Rev. Lett.* **89** 107203
[3] Medvedkin G A, Ishibashi T, Nishi T, Hayata K, Hasegawa Y and Sato K 2000 *Japan. J. Appl. Phys.* **39** L949
[4] Theodoropoulou N, Hebard A F, Overberg M E, Abernathy C R, Pearton S J, Chu S N G and Wilson R G 2001 *Appl. Phys. Lett.* **78** 3475
[5] Reed M L, El-Masry N A, Stadelmaier H H, Ritums M K, Reed M J, Parker C A, Roberts J C and Bedair S M 2001 *Appl. Phys. Lett.* **79** 3473
[6] Matsumoto Y, Murakami M, Shono T, Hasagawa T, Fukumura T, Kawasaki M, Ahmet P, Chikyow T, Koshihara S and Koinuma H 2001 *Science* **291** 854
[7] Ogale S B, Choudhary R J, Buban J P, Lofland S E, Shinde S R, Kale S N, Kulkarni V N, Higgins J, Lanci C, Simpson J R, Browning N D, Das Sarma S, Drew H D, Greene R L and Venkatesan T 2003 *Phys. Rev. Lett.* **91** 077205
[8] Zhao Y G, Shinde S R, Ogale S B, Higgins J, Choudhary R J, Kulkarni V N, Greene R L, Venkatesan T, Lofland S E, Lanci C, Buban J P, Browning N D, Das Sarma S and Millis A J 2003 *Appl. Phys. Lett.* **83** 2199
[9] Matsukura F, Ohno H, Shen A and Sugawara Y 1998 *Phys. Rev.* B **57** R2037
Dietl T, Ohno H, Matsukura F, Cibert J and Ferrand D 2000 *Science* **287** 1019
Konig J, Lin H-H and MacDonald A H 2000 *Phys. Rev. Lett.* **84** 5628
[10] Dietl T, Ohno H, Matsukura F, Cibert J and Ferrand C 2000 *Science* **287** 1019
[11] Sato K, Dederichs P H, Katayama-Yoshida H and Kudrnovsky J 2003 *Physica* B **340–342** 863
Sato K, Dederichs P H, Katayama-Yoshida H and Kudrnovsky J 2004 *J. Phys.: Condens. Matter* **16** S5491
Mahadevan P and Zunger A 2003 *Phys. Rev.* B **68** 075202
[12] Sarma D D 2001 *Curr. Opin. Solid State Mater. Sci.* **5** 261
Sarma D D, Mahadevan P, Saha-Dasgupta T, Ray S and Kumar A 2000 *Phys. Rev. Lett.* **85** 2549
[13] Akai H 1998 *Phys. Rev. Lett.* **81** 3002
Schilfgaarde M and van and Mryasov O N 2001 *Phys. Rev.* B **63** 233205
[14] Dyck J S, Hajek P, Lostak P and Uher C 2002 *Phys. Rev.* B **65** 115212
[15] Miao M S and Lambrecht W R L 2003 *Phys. Rev.* B **68** 125204
[16] Forster R H, Johnston G B and Wheeler D A 1968 *J. Phys. Chem. Solids* **29** 855
[17] De Groot R A, Muller F M, Van Engen P G and Buschow K H J 1983 *Phys. Rev. Lett.* **50** 2024
[18] Xia Y, Bhattacharya S, Ponnambalm V, Pope A L, Poon S J and Tritt T M 2000 *J. Appl. Phys.* **88** 1952
[19] Evers C B H, Richter C G, Hartjes K and Jeitschko W 1997 *J. Alloys Compounds* **252** 93
[20] van Leuken H and de Groot R A 1995 *Phys. Rev. Lett.* **74** 1171
[21] Tobola J, Kaprzyk S and Pecheur P 2003 *Phys. Status Solidi* b **236** 531
[22] Andersen O K and Jepsen O 1984 *Phys. Rev. Lett.* **53** 2571
Jepson O and Andersen O K 2000 *The Stuttgart TB-LMTO-ASA Program, version 47*
[23] Andersen O K, Pawlowska Z and Jepsen O 1986 *Phys. Rev.* B **34** 5253
[24] Pawlowska Z, Christensen N E, Satpathy A and Jepsen O 1986 *Phys. Rev.* B **34** 7080
[25] Nanda B R K and Dasgupta I 2003 *J. Phys.: Condens. Matter* **15** 7307
Nanda B R K and Dasgupta I 2005 *Comput. Mater. Sci.* at press
[26] Dronskowski R and Blochl P E 1993 *J. Phys.: Condens. Matter* **97** 8617
[27] Von Barth U 1972 *J. Phys. C: Solid State Phys.* **5** 1629
Hedin L 1971 *J. Phys. C: Solid State Phys.* **4** 2064
[28] Perdew J P, Burke K and Ernzerhof M 1996 *Phys. Rev. Lett.* **77** 3865
[29] Jepsen O and Andersen O K 1971 *Solid State Commun.* **9** 1763
Blochl P, Jepsen O and Andersen O K 1994 *Phys. Rev.* B **49** 16223
[30] Aliev F G, Brandt N B, Moschalkov V V, Kozyrkov V V, Scolozdra V V and Belogorokhov A I 1990 *Z. Phys.* B **80** 353
[31] Nanda B R K and Dasgupta I 2005 unpublished
[32] Galankis I, Dederichs P H and Papanikolaou N 2002 *Phys. Rev.* B **66** 134428
[33] Anderson P W and Hasegawa H 1955 *Phys. Rev.* **100** 675
[34] Sanyal B, Bengone O and Mirbt S 2003 *Phys. Rev.* B **68** 205210